

LETTERS

Drosophila pink1 is required for mitochondrial function and interacts genetically with *parkin*

Ira E. Clark^{1*}, Mark W. Dodson^{1*}, Changan Jiang^{1*}, Joseph H. Cao¹, Jun R. Huh², Jae Hong Seol³, Soon Ji Yoo⁴, Bruce A. Hay² & Ming Guo¹

Parkinson's disease is the second most common neurodegenerative disorder and is characterized by the degeneration of dopaminergic neurons in the substantia nigra. Mitochondrial dysfunction has been implicated as an important trigger for Parkinson's disease-like pathogenesis because exposure to environmental mitochondrial toxins leads to Parkinson's disease-like pathology¹. Recently, multiple genes mediating familial forms of Parkinson's disease have been identified, including *PTEN-induced kinase 1* (*PINK1*; *PARK6*) and *parkin* (*PARK2*), which are also associated with sporadic forms of Parkinson's disease^{2–6}. *PINK1* encodes a putative serine/threonine kinase with a mitochondrial targeting sequence². So far, no *in vivo* studies have been reported for *pink1* in any model system. Here we show that removal of *Drosophila PINK1* homologue (CG4523; hereafter called *pink1*) function results in male sterility, apoptotic muscle degeneration, defects in mitochondrial morphology and increased sensitivity to multiple stresses including oxidative stress. *Pink1* localizes to mitochondria, and mitochondrial cristae are fragmented in *pink1* mutants. Expression of human *PINK1* in the *Drosophila* testes restores male fertility and normal mitochondrial morphology in a portion of *pink1* mutants, demonstrating functional conservation between human and *Drosophila PINK1*. Loss of *Drosophila parkin* shows phenotypes similar to loss of *pink1* function^{7,8}. Notably, overexpression of *parkin* rescues the male sterility and mitochondrial morphology defects of *pink1* mutants, whereas double mutants removing both *pink1* and *parkin* function show muscle phenotypes identical to those observed in either mutant alone. These observations suggest that *pink1* and *parkin* function, at least in part, in the same pathway, with *pink1* functioning upstream of *parkin*. The role of the *pink1*–*parkin* pathway in regulating mitochondrial function underscores the importance of mitochondrial dysfunction as a central mechanism of Parkinson's disease pathogenesis.

Drosophila melanogaster contains a single *PINK1* homologue (CG4523). As with human *PINK1*, *Drosophila PINK1* has a predicted amino-terminal mitochondrial targeting sequence and a serine/threonine kinase domain that shares 43% amino acid identity and 60% similarity with human *PINK1* (Supplementary Fig. S1a). More than 25 *PINK1* missense and truncating mutations have been found in Parkinson's disease patients^{1,4,6}. Many of the residues altered by missense mutations⁴ are conserved in *Drosophila PINK1* (Supplementary Fig. S1a).

pink1 messenger RNA was detectable at all developmental stages with the highest expression levels in the adult head and testes (Supplementary Fig. S1b). We generated two chromosomal deletions; both showed very similar if not identical phenotypes and

are probably null alleles (Fig. 1a and Supplementary Fig. S1c). Both *pink1* deletion strains were viable; however, they were completely male sterile and almost completely female sterile. Because proper mitochondrial function is required for spermatogenesis, we examined the *pink1* mutant testes for mitochondrial defects. During spermatogenesis, stem-cell differentiation is followed by mitosis and meiosis with incomplete cytokinesis, creating syncytial cysts of 64 spermatids⁹. Subsequently, mitochondria exhibit marked morphological changes. Specifically, early spermatids undergo mitochondrial aggregation and fusion, creating two giant mitochondria that form a spherical structure known as the nebenkern⁹. Under phase contrast microscopy, such 'onion stage' spermatids can be identified as having two adjacent spherical structures: the nucleus and the nebenkern (Fig. 1b). During spermatid elongation, the nebenkern unfurls to yield two mitochondrial derivatives⁹ (Fig. 1i). In *pink1* mutant males, spermatid nuclei appeared normal; however, nebenkerns were vacuolated (Fig. 1d, g) and this vacuolation persisted during subsequent spermatid elongation (Fig. 1k).

To analyse further these mitochondrial defects, we examined *pink1* mutant testes using transmission electron microscopy (TEM). After elongation, spermatids undergo a process known as individualization, in which the cytoplasmic bridges that link the 64 spermatids within a cyst are broken and excess cytoplasm is extruded⁹. After individualization, each spermatid consists largely of the central axoneme, a microtubule-based structure required for motility, and the mitochondrial derivatives, located next to the axoneme (Fig. 1m). Spermatids in *pink1* mutant testes underwent elongation (Fig. 1k); however, numerous defects in individualization were observed (Fig. 1o). Although the number of spermatids in each cyst, the shape and the size of the axoneme, and the spatial relationship between the axoneme and mitochondria were unchanged (Fig. 1o), the overall architecture of *pink1* mutant cysts was disorganized, and the mitochondria were of variable size and were frequently smaller than those in wild-type cysts (Fig. 1, compare panels o and n). *pink1* mutant cysts also frequently contained a large mass of electron-dense material, which may represent aberrant mitochondria (Fig. 1o).

To ensure that the mitochondrial and individualization phenotypes were indeed due to lack of *pink1* function, we generated multiple lines bearing a *pink1* genomic rescue transgene (Fig. 1a). *pink1*⁵ or *pink1*⁹ males carrying a single copy of this transgene were fertile (98% fertile, *n* = 40). Moreover, defects in mitochondrial morphology and individualization were almost completely suppressed (Fig. 1e, h, l, p). Thus, the male sterility phenotype is due to lack of *pink1* function.

To determine the subcellular localization of *Pink1*, we generated a carboxy-terminal *myc*-tagged version of the *pink1* genomic rescue

¹Department of Neurology, Brain Research Institute, The David Geffen School of Medicine, University of California, Los Angeles, California 90095, USA. ²Division of Biology, California Institute of Technology, Pasadena, California 91125, USA. ³Department of Biological Sciences, Seoul National University, Seoul 151-742, Korea. ⁴Department of Biology, Kyung Hee Institute of Age-related and Brains Disease, Kyung Hee University, Seoul 130-701, Korea.

*These authors contributed equally to this work.

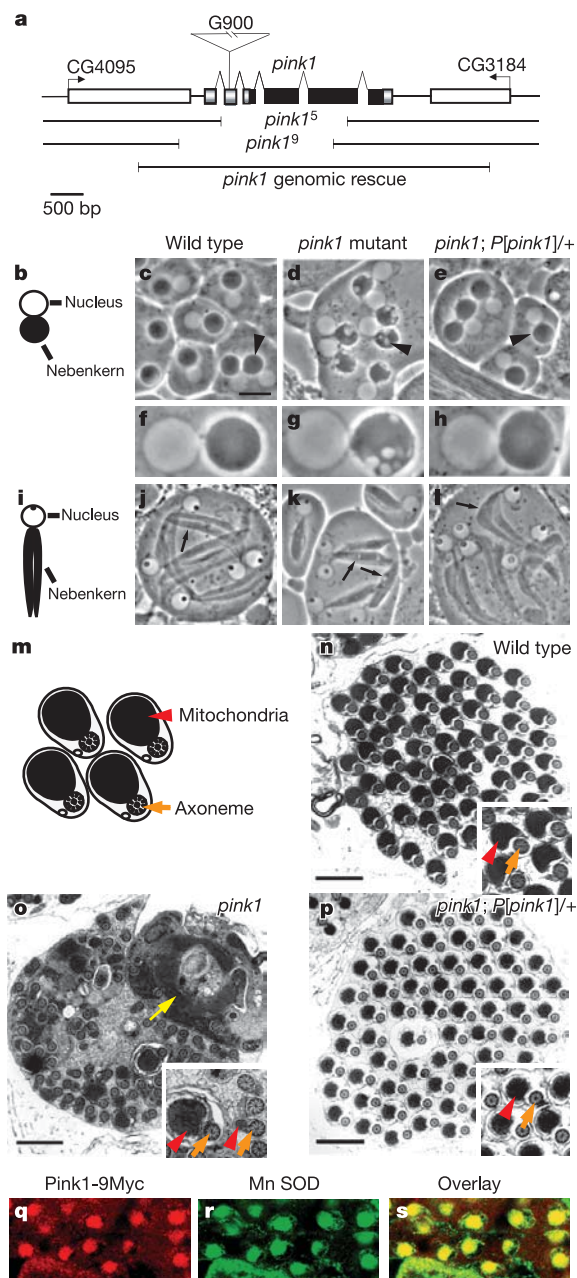


Figure 1 | *pink1* mutants exhibit mitochondrial and individualization defects in spermatids. **a**, Genomic map of *pink1* (cytological location 6C6). P element insertion (triangle), *pink1* coding and untranslated regions (dark and shaded rectangles), and nearby genes (open rectangles) are depicted. The *pink1*⁵ deletion removes the mitochondrial targeting sequence and over 70% of the kinase domain, including motifs required for ATP binding, catalysis and metal binding³⁰. The *pink1*⁹ deletion removes the entire 5' untranslated region (UTR) and part of the kinase domain. The *pink1* genomic rescue construct does not include the full coding region of nearby genes. **b-l**, Schematics and phase contrast micrographs of mitochondrial morphogenesis in spermatids during the 'onion stage' (**b-h**) and spermatid elongation (**i-l**). In both stages, *pink1* mutants show vacuolation of mitochondria (arrowheads and arrows). **m-p**, Schematic and TEM images of single post-individualization cysts containing 64 spermatids. Each spermatid contains an axoneme (orange arrow) and mitochondrial derivative (red arrowhead) within an individual plasma membrane. The *pink1* mutant cyst (**o**) shows individualization defects, mitochondria of variable sizes, and a mass of electron-dense material (yellow arrow). **q-s**, Double labelling of *pink1-9myc* testes with anti-Myc (**q**) and anti-Mn SOD (**r**) demonstrates that Pink1 is localized to the nebenkerns. Scale bars: 10 μ m (**c-e**, **j-l**), 4 μ m (**f-h**) and 1 μ m (**n-p**).

transgene. *pink1* mutant males with the *pink1-9myc* transgene were fertile (100%, $n = 30$), suggesting that the Myc tag does not interfere with Pink1 function. Immunofluorescence on *pink1-9myc* testes demonstrated that Pink1-9Myc protein co-localized to nebenkerns with manganese superoxide dismutase (Mn SOD), a mitochondrial marker¹⁰ (Fig. 1q-s). Together, these observations suggest that *pink1* functions in spermatogenesis to regulate mitochondrial morphology and function.

To determine whether *pink1* has a more general role in mitochondrial function, we examined other tissues in *pink1* mutants. We were unable to detect a significant change in the number of dopaminergic neurons between *pink1* mutant and wild-type flies at 50 days old (Supplementary Fig. S2). However, striking phenotypes were observed in muscle, which also has high energy demands requiring robust mitochondrial function. *pink1* mutants have 'held-up' wings (Fig. 2e) and poor flight performance (Supplementary Fig. S3), suggesting a defect in indirect flight muscles. In wild-type adults, muscle fibres were well organized in parallel stripes with regular banding and no vacuolation (Fig. 2b). In contrast, muscle fibres from age-matched 14-day-old *pink1* mutants were disorganized with prominent vacuoles (Fig. 2f). Ultrastructural TEM analysis showed that the mitochondrial cristae were fragmented in *pink1* mutants, with some mitochondria appearing nearly hollow (Fig. 2g, h), as compared to wild-type mitochondria, which were filled with densely packed cristae (Fig. 2c, d). All of these phenotypes were fully suppressed by the *pink1* genomic rescue transgene (Fig. 2i-l and Supplementary Fig. S3). Previous immuno-electron microscopy studies have shown that mammalian PINK1 is localized to mitochondrial cristae¹¹.

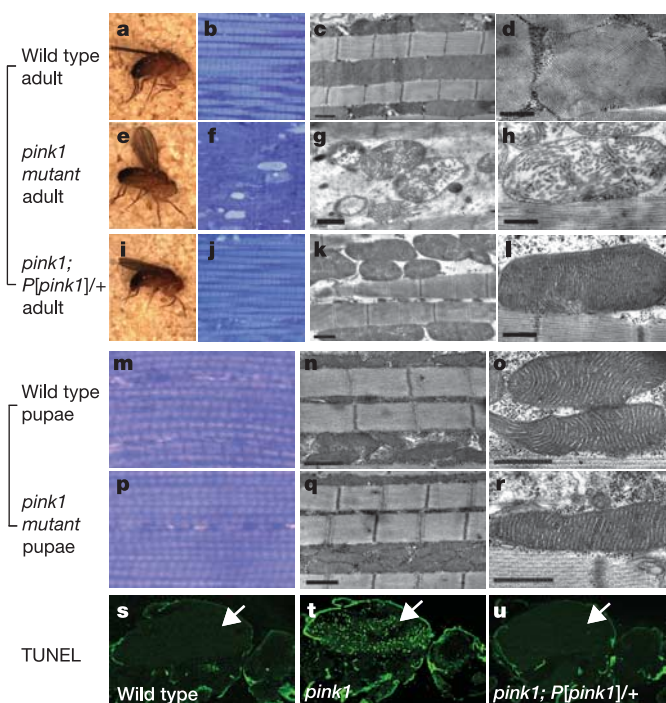


Figure 2 | *pink1* mutants undergo apoptotic muscle degeneration and fragmentation of mitochondrial cristae. *pink1* mutants have held-up wings (compare panels **a** and **e**). **b-d**, **f-h**, **j-l**, Toluidine blue staining (**b**, **f**, **j**) and TEMs (**c**, **d**, **g**, **h**, **k**, **l**) of indirect flight muscle from 14-day-old flies. Muscles of *pink1* mutants show numerous vacuoles (compare **f** and **b**) and mitochondria with fragmented cristae (compare **g**, **h** with **c**, **d**). **m-r**, At 96 h after puparium formation, *pink1* mutant muscle fibres and mitochondria appear normal (compare **p-r** and **m-o**). *pink1*⁵ mutants show many TUNEL-positive nuclei in indirect flight muscle (compare **t** and **s**). Each of these mutant phenotypes is rescued by the *pink1* genomic rescue transgene (**i-l**, **u**). Scale bars: 1.0 μ m (**c**, **g**, **k**, **n**, **q**) and 0.5 μ m (**d**, **h**, **l**, **o**, **r**).

Together, these observations suggest that mitochondrial cristae are a site of Pink1 action, either directly or indirectly.

To investigate whether these muscle phenotypes are developmental or degenerative, we examined indirect flight muscles in *pink1* mutants during development and shortly after eclosion. At 96 h after puparium formation, muscle and mitochondrial morphology of *pink1* mutants (Fig. 2p–r) was indistinguishable from that of age-matched wild-type flies (Fig. 2m–o). At 1–2 days after eclosion, however, *pink1* mutants already showed muscle degeneration and fragmentation of mitochondrial cristae (see below), which was completely suppressed by the *pink1* genomic rescue transgene (data not shown). Furthermore, indirect flight muscles from *pink1* mutants 1–2 days after eclosion demonstrated a marked increase in TdT-mediated dUTP nick end labelling (TUNEL)-positive nuclei (Fig. 2s, t). Taken together, these findings suggest that muscle phenotypes of *pink1* mutants are rapidly degenerative and apoptotic in nature. Finally, ATP levels in *pink1* mutants were significantly reduced (Fig. 3f), demonstrating that mitochondrial function is also severely affected by loss of *pink1*. Apoptosis and reduced ATP levels in *pink1* mutants were fully suppressed by the *pink1* genomic rescue transgene (Figs 2u and 3f).

Mitochondrial dysfunction can lead to decreased resistance to reactive oxygen species, which has been implicated in Parkinson's disease pathogenesis. Sensitivity to reactive oxygen species has also been observed in flies lacking either *parkin*⁸ or *DJ-1*^{12–15}, another familial Parkinson's disease gene¹⁶. To explore the role of *pink1* in resistance to oxidative stress, we analysed the survival of *pink1* mutants after exposure to paraquat, a free radical inducer, or rotenone, which impairs complex I activity in the mitochondrial respiratory chain. Both agents can induce Parkinson's disease-like

pathology in mammals¹⁷. To avoid variability due to genetic background, we included two control strains: a wild-type line with chromosomal background identical to that in *pink1* mutants (precise excision), and a line of *pink1* mutants with the genomic rescue transgene. *pink1* mutants showed 59% reduced resistance to paraquat, and 71% reduced resistance to rotenone (Fig. 3a, b). *pink1* mutants were also sensitive to a hyperoxic environment, a stress that does not rely on feeding (data not shown). The stress sensitivity of *pink1* mutants was not limited to oxidative stress, however, as they were also sensitive to dithiothreitol (DTT), a protein folding inhibitor, and high concentrations of salt, an osmotic stress (Fig. 3c, d). Finally, *pink1* mutants were shorter lived. At 56 days, only 12% of *pink1* mutants were alive, compared with 70–80% of wild-type flies and *pink1* mutants with the *pink1* genomic rescue transgene (Fig. 3e). The sensitivity to multiple stresses in *pink1* mutants may reflect a generalized sickness or may be a consequence of mitochondrial dysfunction.

Drosophila Pink1 shares significant homology with human PINK1 (Supplementary Fig. S1a). To test functional conservation of the human and *Drosophila* homologues, we investigated whether human PINK1 could rescue fly *pink1* mutant phenotypes. We expressed human PINK1 using the testes-specific $\beta 2$ -tubulin promoter¹⁸ (TMR-human PINK1), which is expressed in developing spermatids beginning just before the onion stage. Fertility was restored in 17% ($n = 93$) of *pink1* mutant males carrying the TMR-human PINK1 transgene and mitochondrial phenotypes were rescued in these fertile males (Fig. 4; compare panels b and e with a and d). Thus, *Drosophila* and human Pink1 share at least some functional conservation.

parkin mutants show phenotypes similar to *pink1* mutants: male sterility, apoptotic muscle degeneration, fragmentation of mitochondrial cristae and sensitivity to multiple stresses including oxidative stress^{7,8}. We explored whether *pink1* and *parkin* function in the same genetic pathway. First, we determined whether *parkin* overexpression

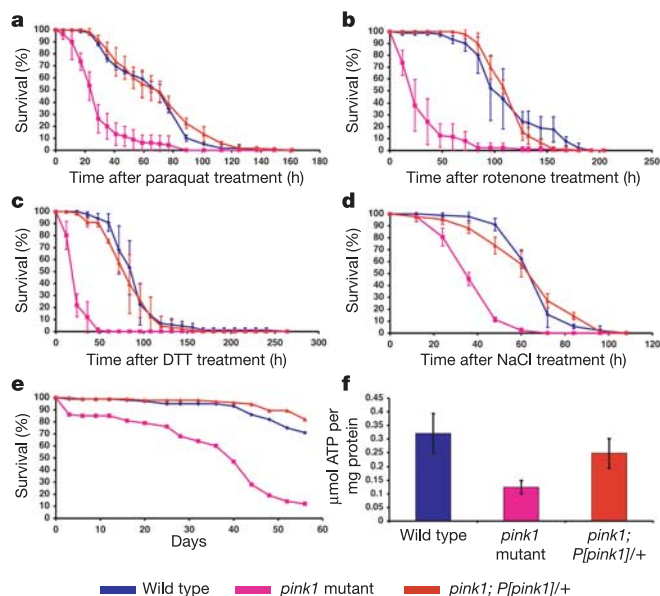


Figure 3 | *pink1* mutants are sensitive to multiple stresses, and have reduced lifespan and ATP levels. a–d, Survival of *pink1*⁵ mutants (pink), wild type (precise excision, blue) and *pink1*⁵ mutants with the genomic rescue transgene (red) after exposure to 20 mM paraquat (a), 5 mM rotenone (b), 100 mM DTT (c) and 500 mM NaCl (d). Mean survival times (in hours) for *pink1*⁵, wild-type and *pink1*⁵; *P[pink1]*+/+ flies, respectively, are: paraquat 29.0 ± 6.8, 65.7 ± 1.0 and 70.8 ± 5.5; rotenone 33.6 ± 11.6, 115 ± 14.3 and 116.2 ± 3.6; DTT 25.8 ± 4, 92.4 ± 12.6 and 84.4 ± 9.8; NaCl 40.5 ± 1.5, 68.8 ± 1.8 and 66.6 ± 1.9. e, *pink1*⁵ mutants have reduced lifespan. f, Mean ATP levels (μmol mg⁻¹ protein) of *pink1*⁵ mutants (0.13 ± 0.02) are significantly reduced, as compared with wild-type (precise excision, 0.32 ± 0.07; $P < 0.02$) and *pink1*⁵ flies with the rescue transgene (0.25 ± 0.05; $P < 0.05$). Error bars indicate standard deviation. Student's *t*-test was used.

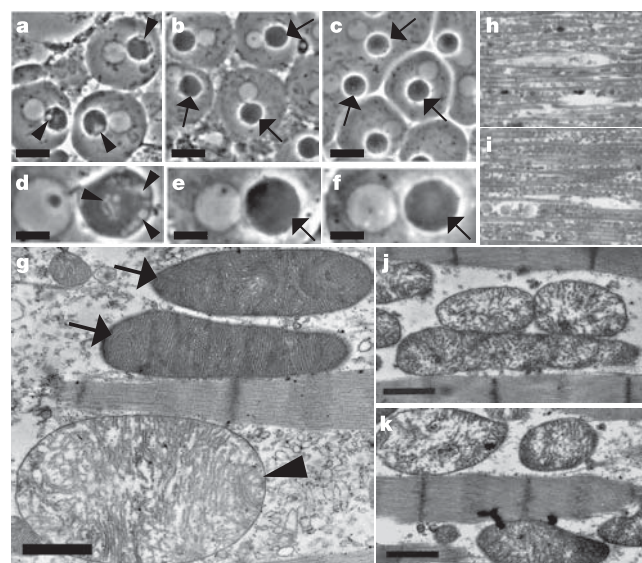


Figure 4 | Fly *pink1* is functionally conserved with human PINK1, and acts upstream of *parkin*. a–f, Onion-stage testes. The vacuolation of nebenspermatids (arrowheads) in *pink1*⁵ testes (a, d) is almost completely suppressed (arrows) by the TMR-human PINK1 (b, e) and TMR-*parkin* (c, f) transgenes. g, Overexpression of *parkin* in muscle suppresses the *pink1* mutant phenotype; some mitochondria contain densely packed cristae (arrows), whereas others (arrowhead) still contain fragmented cristae. h–k, Toluidine blue staining (h, i) and TEM (j, k) of 2-day-old adult indirect flight muscles. Double mutants of *pink1* and *parkin* show muscle (i) and mitochondria (k) phenotypes identical to those of *pink1* (h, j) or *parkin* single mutants^{7,8} (data not shown). Scale bars: 10 μm (a–c), 4 μm (d–f) and 1.0 μm (g, j, k).

in *pink1* mutant testes could compensate for loss of *pink1* function and restore male fertility. If *parkin* positively regulates *pink1*, we would expect that overexpression of *parkin* would still result in the *pink1* null phenotype and thus be sterile. Conversely, if *parkin* acts downstream of *pink1*, overexpression of *parkin* might suppress the *pink1* null phenotype and restore fertility. *parkin* overexpression in *pink1* mutants resulted in significant suppression of sterility (62% fertile, $n = 65$) and mitochondrial phenotype (Fig. 4; compare panels c and f with a and d). In contrast, overexpression of *pink1* in the *parkin*^{Δ21} null background⁸ failed to suppress sterility due to lack of *parkin* (0% fertile, $n = 60$). As controls, TMR-*pink1* and TMR-*parkin* restored the fertility in *pink1* and *parkin* mutants, respectively (100% fertile, $n = 40$; 97% fertile, $n = 40$, respectively). Second, when *parkin* was specifically expressed in *pink1* mutant muscle using the UAS/GAL4 system¹⁹, a subset of 1–2-day-old flies contained mitochondria with densely packed cristae (Fig. 4g), which was never seen in age-matched *pink1* mutants (Fig. 4j). When *pink1* was specifically expressed in *pink1* mutant muscle, normal mitochondrial morphology was restored (data not shown). The incomplete rescue in mitochondrial morphology seen with *parkin* overexpression in indirect flight muscles may reflect low expression levels of the transgene. Alternatively, *parkin* overexpression may bypass the requirement for only a subset of *pink1* functions. In either case, these results suggest that *parkin* acts downstream of *pink1*, although it is formally possible that they act in parallel on shared targets.

To test further this hypothesis, we generated double mutants that removed both *pink1* and *parkin* function. If *pink1* and *parkin* act in a linear pathway, double mutants should show phenotypes similar to those observed in either mutant alone. Conversely, if these genes function in parallel pathways to regulate a common process, double mutants would show phenotypes stronger than those of either mutant alone. Double mutants removing both *pink1* and *parkin* function showed mitochondrial and muscle degeneration phenotypes identical to those of either single mutant (Fig. 4h–k and data not shown). Together, these experiments suggest that *parkin* acts, at least in part, downstream of *pink1*. This conclusion is particularly interesting in light of recent work demonstrating that clinical presentations of Parkinson's disease patients harbouring *pink1* or *parkin* mutations are indistinguishable².

Although mild dopaminergic neuronal loss has been observed in *parkin* mutants²⁰, we failed to observe any dopaminergic neuronal loss in *pink1* mutants. Similarly, knockout mice for *parkin* and *DJ-1* generated by multiple groups fail to show any dopaminergic neuronal loss, although functional impairments of the nigrostriatal system and mitochondrial dysfunction have been observed^{21,22}. It is possible that a more sensitive assay, such as mitochondrial morphology or function, or dopaminergic neuronal physiology, may reveal a defect in dopaminergic neurons in *pink1* mutants. However, it is important to note that Parkinson's disease is a multi-system disease affecting more than dopaminergic neurons. Degeneration of many non-dopaminergic neurons including olfactory and brain stem neurons predates that of dopaminergic neurons²³. Moreover, pathological changes and defects in mitochondrial respiratory chain function have been observed in muscle biopsies of Parkinson's disease patients^{24–26}, suggesting more global pathology in Parkinson's disease. Our finding that *pink1* acts upstream of *parkin* to regulate mitochondria strengthens the accumulating evidence that *parkin* has an important role in mitochondrial function, and underscores mitochondrial dysfunction as a central mechanism for Parkinson's disease pathogenesis. The *pink1*–*parkin* pathway provides an entry point for isolating other genes related to regulation of mitochondria, which may include components that function in Parkinson's disease pathogenesis.

METHODS

Molecular biology. To express genes specifically in testes during spermatid differentiation, the pGMR vector²⁷ was modified to replace the glass-binding

sites with part of the regulatory region of $\beta 2$ -tubulin¹⁸, yielding pTMR ($\beta 2$ -tubulin mediated expression).

Genetics and *Drosophila* strains. *pink1* deletions were generated by imprecise excision of the G900 P element obtained from GenExel, which is viable and fertile. Breakpoints were mapped by genomic polymerase chain reaction (PCR) followed by sequencing. For muscle rescue experiments, UAS-*pink1* or UAS-*parkin* was driven by 24B-GAL4 in the *pink1*⁵ mutant background.

Immunofluorescence and confocal microscopy. We used the following antibodies: mouse anti-Myc (Upstate, 1:400), rabbit anti-Mn SOD (Stressgen, 1:300), mouse anti-tyrosine hydroxylase (Immunostar, 1:300).

Light and electron microscopy. For light and electron microscopic analyses, testes were prepared as described previously (refs 9 and 28, respectively). For muscle TEM, thoraces were fixed in paraformaldehyde/glutaraldehyde, post-fixed in osmium tetroxide, dehydrated and embedded in Epon. One-micrometre sections were stained with Toluidine blue, and 50–80-nm sections with uranyl acetate and lead citrate. At least three testes or thoraces of each genotype were examined by TEM.

Stress, flight and longevity assays. 0–3-day-old males were anaesthetized on ice, aged for 48 h, starved for 6 h and subjected to 5% sucrose plus each agent. Three vials of 30–40 flies were assayed simultaneously for each genotype. Flight assays were performed in three groups of 40 3–4-day-old flies, as described previously²⁹. For longevity measurements, 100 males of each genotype were divided into five vials. Flies were maintained at 25 °C and transferred to fresh food every 3–4 days.

ATP and TUNEL assays. For each genotype, ATP levels were determined from lysates of three groups of five 2–4-day-old flies using the ATP bioluminescence assay kit HS II from Roche. Values were normalized to protein content measured by the Bio-Rad protein assay reagent. TUNEL assays were carried out on cryostat sections using the *in situ* cell death detection kit from Roche.

Received 15 February; accepted 7 April 2006.

Published online 30 April 2006.

- Moore, D. J., West, A. B., Dawson, V. L. & Dawson, T. M. Molecular pathophysiology of Parkinson's disease. *Annu. Rev. Neurosci.* **28**, 57–87 (2005).
- Valente, E. M. et al. Hereditary early-onset Parkinson's disease caused by mutations in PINK1. *Science* **304**, 1158–1160 (2004).
- Kitada, T. et al. Mutations in the *parkin* gene cause autosomal recessive juvenile parkinsonism. *Nature* **392**, 605–608 (1998).
- Bonifati, V. et al. Early-onset parkinsonism associated with PINK1 mutations: frequency, genotypes, and phenotypes. *Neurology* **65**, 87–95 (2005).
- Klein, C. et al. PINK1, Parkin, and DJ-1 mutations in Italian patients with early-onset parkinsonism. *Eur. J. Hum. Genet.* **13**, 1086–1093 (2005).
- Ibanez, P. et al. Mutational analysis of the PINK1 gene in early-onset parkinsonism in Europe and North Africa. *Brain* **129**, 686–694 (2006).
- Greene, J. C. et al. Mitochondrial pathology and apoptotic muscle degeneration in *Drosophila parkin* mutants. *Proc. Natl Acad. Sci. USA* **100**, 4078–4083 (2003).
- Pesah, Y. et al. *Drosophila parkin* mutants have decreased mass and cell size and increased sensitivity to oxygen radical stress. *Development* **131**, 2183–2194 (2004).
- Fuller, M. T. in *The Development of Drosophila melanogaster* 71–147 (Cold Spring Harbor Laboratory Press, Cold Spring Harbor, New York, 1993).
- Van Steeg, H., Oudshoorn, P., Van Hell, B., Polman, J. E. & Grivell, L. A. Targeting efficiency of a mitochondrial pre-sequence is dependent on the passenger protein. *EMBO J.* **5**, 3643–3650 (1986).
- Silvestri, L. et al. Mitochondrial import and enzymatic activity of PINK1 mutants associated to recessive parkinsonism. *Hum. Mol. Genet.* **14**, 3477–3492 (2005).
- Meulener, M. et al. *Drosophila DJ-1* mutants are selectively sensitive to environmental toxins associated with Parkinson's disease. *Curr. Biol.* **15**, 1572–1577 (2005).
- Menzies, F. M., Yenissetti, S. C. & Min, K. T. Roles of *Drosophila DJ-1* in survival of dopaminergic neurons and oxidative stress. *Curr. Biol.* **15**, 1578–1582 (2005).
- Yang, Y. et al. Inactivation of *Drosophila DJ-1* leads to impairments of oxidative stress response and phosphatidylinositol 3-kinase/Akt signaling. *Proc. Natl Acad. Sci. USA* **102**, 13670–13675 (2005).
- Park, J. et al. *Drosophila DJ-1* mutants show oxidative stress-sensitive locomotor dysfunction. *Gene* **361**, 133–139 (2005).
- Bonifati, V. et al. Mutations in the DJ-1 gene associated with autosomal recessive early-onset Parkinsonism. *Science* **299**, 256–259 (2003).
- Przedborski, S. & Ischiropoulos, H. Reactive oxygen and nitrogen species: weapons of neuronal destruction in models of Parkinson's disease. *Antioxid. Redox Signal.* **7**, 685–693 (2005).
- Huh, J. R. et al. Multiple apoptotic caspase cascades are required in nonapoptotic roles for *Drosophila* spermatid individualization. *PLoS Biol.* **2**, E15 (2004).
- Brand, A. H. & Perrimon, N. Targeted gene expression as a means of altering cell fates and generating dominant phenotypes. *Development* **118**, 401–415 (1993).
- Whitworth, A. J. et al. Increased glutathione S-transferase activity rescues dopaminergic neuron loss in a *Drosophila* model of Parkinson's disease. *Proc. Natl Acad. Sci. USA* **102**, 8024–8029 (2005).

21. Fleming, S. M., Fernagut, P. O. & Chesselet, M. F. Genetic mouse models of parkinsonism: strengths and limitations. *NeuroRx* **2**, 495–503 (2005).
22. Palacino, J. J. *et al.* Mitochondrial dysfunction and oxidative damage in parkin-deficient mice. *J. Biol. Chem.* **279**, 18614–18622 (2004).
23. Braak, H. *et al.* Staging of brain pathology related to sporadic Parkinson's disease. *Neurobiol. Aging* **24**, 197–211 (2003).
24. Ahlqvist, G., Landin, S. & Wroblewski, R. Ultrastructure of skeletal muscle in patients with Parkinson's disease and upper motor lesions. *Lab. Invest.* **32**, 673–679 (1975).
25. Bindoff, L. A., Birch-Machin, M. A., Cartledge, N. E., Parker, W. D. Jr & Turnbull, D. M. Respiratory chain abnormalities in skeletal muscle from patients with Parkinson's disease. *J. Neurol. Sci.* **104**, 203–208 (1991).
26. Wiedemann, F. R., Winkler, K., Lins, H., Wallesch, C. W. & Kunz, W. S. Detection of respiratory chain defects in cultivated skin fibroblasts and skeletal muscle of patients with Parkinson's disease. *Ann. NY Acad. Sci.* **893**, 426–429 (1999).
27. Hay, B. A., Wolff, T. & Rubin, G. M. Expression of baculovirus P35 prevents cell death in *Drosophila*. *Development* **120**, 2121–2129 (1994).
28. Tokuyasu, K. T., Peacock, W. J. & Hardy, R. W. Dynamics of spermiogenesis in *Drosophila melanogaster*. I. Individualization process. *Z. Zellforsch. Mikrosk. Anat.* **124**, 479–506 (1972).
29. Benzer, S. Genetic dissection of behaviour. *Sci. Am.* **229**, 24–37 (1973).
30. Hanks, S. K. & Hunter, T. Protein kinases 6. The eukaryotic protein kinase superfamily: kinase (catalytic) domain structure and classification. *FASEB J.* **9**, 576–596 (1995).

Supplementary Information is linked to the online version of the paper at www.nature.com/nature.

Acknowledgements We thank G. Mardon and L. Pallanck for *parkin* cDNA and mutant flies; A. Simon, D. Walker, X. Zhan and A. Kiger for technical advice; L. Zipursky, L. Toro and D. Krantz for access to equipment and space; Guo laboratory members for discussions; and the EM core facilities at UCLA Brain Research Institute and at Caltech. We are indebted to R. Young in Seymour Benzer's laboratory for assistance with EM, and F. Laski for his phase contrast microscope. This work was supported by a National Institute of Health (NIH) grant to B.A.H. and an Alfred P. Sloan Foundation Fellowship in Neuroscience and a NIH grant to M.G.

Author Contributions I.E.C., M.W.D., C.J. and J.H.C. in the Guo laboratory conceived and performed the experiments. J.R.H. and B.A.H. in the Hay laboratory assisted with experiments involving TEM in testes and with TUNEL staining; J.H.S. and S.J.Y. provided crucial reagents; and M.G. conceived and performed experiments, supervised the work, and wrote the manuscript with helpful comments from B.A.H. and authors from the Guo laboratory.

Author Information Reprints and permissions information is available at npg.nature.com/reprintsandpermissions. The authors declare no competing financial interests. Correspondence and requests for materials should be addressed to M.G. (mingfly@ucla.edu).